Optical nanomanipulation and structured-beam optical traps

Vincent R. Daria[1] and Woei Ming Lee[1,2,3]

[1] John Curtin School of Medical Research, The Australian National University, Canberra, Australia
[2] Research School of Engineering, The Australian National University, Canberra, Australia
[3] Australia Research Council Centre of Excellence in Advanced Molecular Imaging, Australian National University, Australia.

Introduction

Optical trapping has led to many seminal works on light-matter interactions [1,2]. When light impinges onto small particles, the transfer of photon momentum brings about mechanical forces, in the order of tens of pico-Newton, which is sufficient to influence the physical location of the particle [3]. For particles much smaller than the wavelength of the trapping light, the momentum transfer sets up induced dipole forces with energy inversely proportional to the gradient of external field and, thus, minimum at the focus [4]. The use of dipole forces in optical traps with magnetic fields has been used to localize and cool an ensemble of atoms to create Bose-Einstein condensates [5-7]. **Figure 1** summarizes the mechanical forces experienced by dielectric and metallic particles within the region of the laser's focus. The net mechanical force in an optical trap, F_{OT}, can be decoupled into scattering force (F_s) and gradient force (F_g) with,

$$F_{OT} = F_s + F_g. \tag{1}$$

In **Fig. 1a**, F_s refers to the reaction force set by photons reflecting at the surface of the dielectric particle with a refractive index greater than the surrounding medium ($n_1 > n_o$). F_s tends to push the particle along the direction of light propagation. The transfer of linear momentum for such interaction is therefore dependent on the magnitude of the intensity of the trapping light field. On the other hand, F_g, results from the intensity gradient experienced by the particle when light refracts through the particle. The intensity gradient of a focused laser has a two-dimensional (2D) intensity distribution that takes a form of a bell-shaped

Gaussian profile. When the particle is near the focus, a net force, F_{OT}, pulls the particle to the region of highest intensity (or to the focus) where it tends to reside at its equilibrium position. **Fig. 1b** shows the gradient force along the axial direction. The intensity gradient along the beam propagation imposes a force along the axial plane F_g. The F_g counters F_s from pushing the particle in the direction of light propagation and sets the particle to an equilibrium position along the z-axis.

By satisfying the forces in all three dimensions (3D), a complete optical tweezers is formed. Such a 3D trap requires a high numerical aperture (NA) objective lens. The fine balance of optical forces within a trapped particle is crucial to form a stable 3D optical trap. Particles trapped in 3D are confined at its equilibrium position within the focus of the trapping laser. However, the stability of the particle is only a few hundred nanometers due to thermal forces (Brownian motion). Converting an optical trap into a highly accurate force measurement system requires an understanding of the underlying physical principles relating particle dynamics and Brownian motion. The crucial tenet is that the optically trapped particle may be modelled as a nearly ideal overdamped harmonic oscillator. For a given type of particle (size, dielectric constant, polarizability), a trapped particle experiences a restoring force that is linearly proportional (to a certain degree) to the distance away from center of the optical trap. This linear restoring force is akin to a miniscule spring that obeys Hooke's law i.e. harmonic oscillator. **Figure 1c** illustrates the spring model and the relative spatial distributions of the equilibrium energies along transverse and axial directions where a particle is pulled towards the equilibrium position (lowest energy).
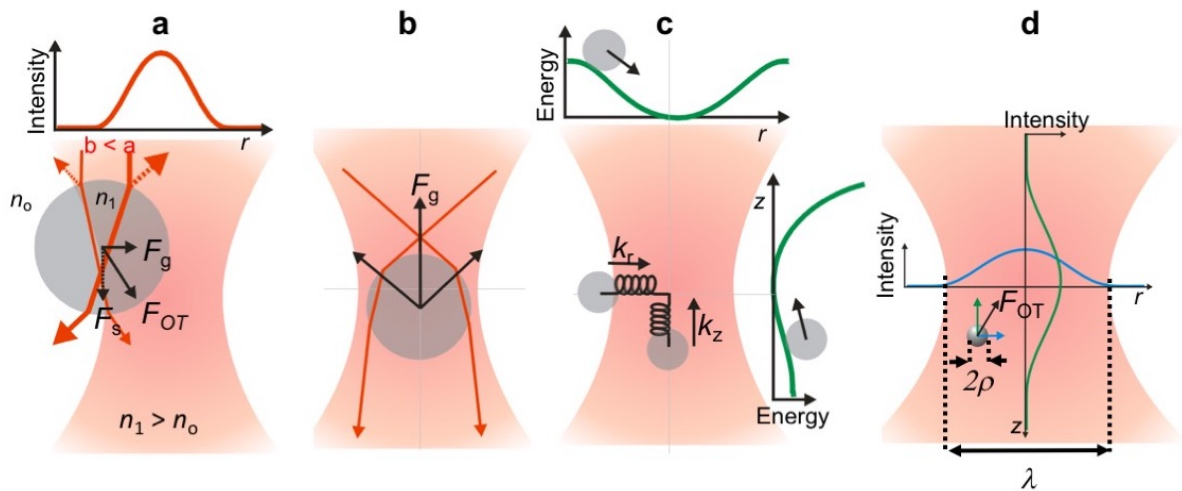

Figure 1. Principle of optical trapping of dielectric particles with index of refraction greater than the surrounding medium, $n_1 > n_o$. (**a**) Scattering and gradient forces (F_s and F_g, respectively) acting on a particle near the beam focus. (**b**). Gradient force along the axial direction that allows trapping the particle in 3D. The balance between axial F_g and F_s should be satisfied to prevent the particle from being pushed by radiation pressure. (**c**) The optical trap visualized as a harmonic oscillator with spring constant, k_r and k_z along the transverse and axial direction, respectively. (**d**) Gradient and dipole forces acting on a nanoparticle with radius, ρ, in a diffraction-limited focused laser beam with wavelength, λ.

In an optical trap, nanoscale particles (or nanoparticles much smaller than λ) act to minimize its energy that corresponds to the electromagnetic field gradient created by the focused Gaussian beam [8,9]. The forces imposed onto a nanoparticle can be considered as a point dipole where the net force, F_{OT}, is the sum of forces given by:

$$F_{OT} = F_s + F_g = \frac{I\sigma n_o}{c} + \frac{2\pi\alpha}{cn_o^2}\nabla I \qquad (2)$$

where α denotes the polarizability of the nanoparticle which for a standard non-absorbing dielectric object is proportional to its volume and equal to $\alpha = n_o^2 \rho^3 (m^2 - 1)/(m^2 + 2)$, $\sigma = (128\pi^5 \rho^6 / 3\lambda^4)(m^2 - 1)^2/(m^2 + 2)^2$ is the scattering cross section of the sphere, ρ is the particle radius, I is the intensity, n_o is the refractive index of the surrounding medium, c denotes the speed of light, m refers to the ratio of the refractive indices (n_1/n_o) and λ is the wavelength of the trapping laser. As such, the scattering forces are directly proportional to the laser intensity and the gradient (or dipole) forces upon the object are due to the inhomogeneous field gradient created by focusing the Gaussian beam to its diffraction limited spot through a high NA (>1) objective lens [10-12]. **Figure 1d** illustrates how the 3D intensity gradient $\nabla I = \frac{\partial I}{\partial x}\boldsymbol{i} + \frac{\partial I}{\partial y}\boldsymbol{j} + \frac{\partial I}{\partial z}\boldsymbol{k}$ of a focused Gaussian beam (along the transverse, $r = \sqrt{x^2 + y^2}$, and axial, z, directions) sets up $\boldsymbol{F}_{OT}$ that traps the particle towards the region of highest intensity. A nanoparticle is shown to be drawn towards the region of highest intensity due to 3D field gradient and dipole forces.

The Generalized Lorenz–Mie scattering theory (GLMT) can bridge the gap between the Rayleigh (dipole) and Mie regimes (ray optics). GLMT describes the scattering of a plane wave by a sphere under a Gaussian beam illumination. The incident field is expanded in terms of constituent plane waves, enabling apodization and aberration transformations (due to the high numerical aperture microscope objective) to be incorporated to theoretically model $\boldsymbol{F}_{OT}$ [13, 14]. The theory can be extended to particles of different geometrical shapes [15]. Barton and co-workers [16,17] derived a fifth order correction to the focused Gaussian beam in order to compute the forces using the Maxwell stress tensor approach. Rohrbach and Stelzer [18] extended the Rayleigh theory to make it valid for large particles by including second-order scattering terms (based on Mie scattering). The vast majority of optical trapping experiments are performed, where the particle diameter is comparable to the wavelength of the trapping laser. Rohrbach later used the Lorentz force density to estimate the trapping forces and found good agreement between theory and experimental measurements [19].

Light's ability to trap both Rayleigh and Mie particles relies on the 3D spatial profile and parameters characterizing the optical field. In a conventional optical trap, focusing a laser beam will provide a stable trap for Mie particles with higher refractive index than the surrounding medium. However, for non-transparent Mie particles or those with lower refractive index where $\boldsymbol{F}_s$ dominates or whose $\boldsymbol{F}_g$ repels the particles from region of higher intensities, a ring-shaped optical field pattern is used to effectively trap or induce linear momentum transfer [20-26]. Thus, shaping the beam distribution will provide more flexible trapping condition. In fact, the induced forces in optical traps with a weakly focused laser as compared to a strongly focused laser are very different. **Figure 2** shows different trapping conditions for different beam profiles. Using a weakly focused beam from a low NA objective lens (**Fig. 3a**) results in a shallow potential well making it difficult to balance the forces. In most instances, the particle is pushed along the propagation axis of the laser beam with $\boldsymbol{F}_s > \boldsymbol{F}_g$. On the other hand, using a high NA objective lens to deliver a strongly focused beam (**Fig. 2b**) with a steep intensity gradient along the axial direction balances both $\boldsymbol{F}_s$ and $\boldsymbol{F}_g$ to keep the particle trapped in 3D. Metallic microparticles reflect light bringing about a strong axial $\boldsymbol{F}_s$ along the propagation of the Gaussian beam [27]. When the particle has a lower refractive index compared to the surrounding medium, a strong repulsive $\boldsymbol{F}_g$ is induced (**Fig. 2c**)[28]. Trapping hollow microbeads or low-index particles with optical vortices [22-24] or dark optical traps [25-26] makes it easier to obtain an equilibrium position, where the beads sit stably within the dark core(**Fig. 3d**).

Thus, tailoring the profile and parameters of an optical field provides optimal conditions for effective use of light's momentum for optical trapping. In the same way, tailored optical

fields that split up a single laser into multiple trapping potentials open up opportunities for studying multiple particle interactions. The holographic and generalized phase contrast methods are complementary techniques that project dynamic arrays of trapping potentials capable of simultaneous manipulation of several particles [25-35]. In addition to optical trapping, tailoring the optical field to produce beams with orbital angular momentum (OAM) with ring-shaped intensity and helical phase profile (or otherwise referred to as optical vortex) has been used to rotate single microscopic particles around a circular orbit [36-38]. Previous works attribute the transfer of OAM to microscopic dielectric particles to a tangential scattering force, which pushes the particles around a vortex[20]. An optical vortex is projected at the focus of a lens by imparting a helical phase pattern on the incident beam. The helical pitch is defined by the topological charge much like Laguerre–Gaussian (LG) beams where the Poynting vector has an azimuthal component, which results to an OAM along the optical axis [39].

In the succeeding sections, we will discuss applications of optical trapping of various particles ranging from nanoparticles to micron sized dielectric particles. We start by discussing far-field optical trapping of single molecules, deoxyribonucleic acid (DNA), quantum dots, nanowires to particles exhibiting nonlinear Kerr effects. We then move to discussing ways to obtain structured light and how we can use these light patterns for optical manipulation of particles. We first discuss its implications in far field optical trapping then move on to near-field optical trapping. In the near-field regime, optical manipulation was initially achieved via evanescent waves on surfaces and metallic tips that are smaller than the diffraction limit. We also discuss recent works on the interaction of nanoparticles with metallic surfaces excited at resonant conditions where the oscillation of electron density excites surface plasmon polaritons. Moreover, trapping metallic nanoparticles using a trapping laser with a resonant wavelength that excites surface plasmons points to several applications in targeted thermal stimulation of cells. We conclude this chapter by discussing future applications to neurobiology.
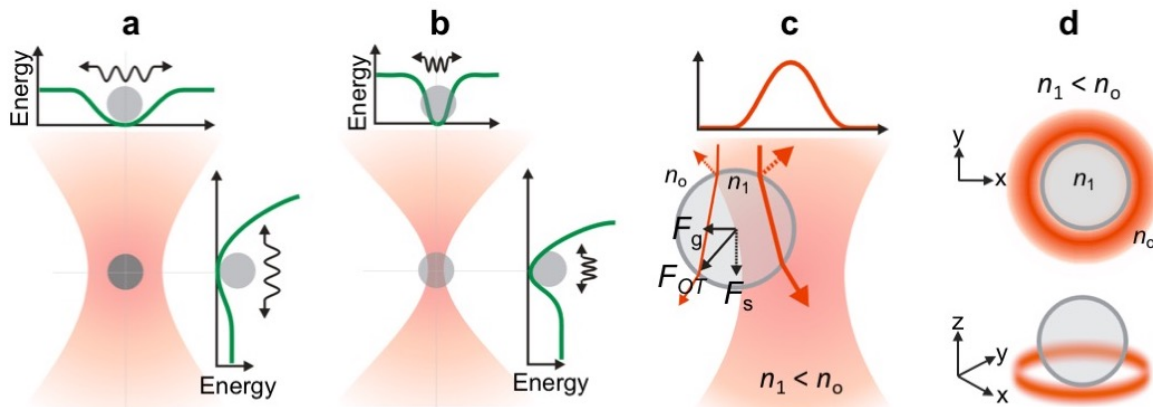

Figure 2. Optical trapping conditions for different spatial distributions of the light. (**a**) A loosely-focused laser produces less stable optical traps as compared to (**b**) tightly focused light. (**c**) Forces acting on a hollow glass (low-index) particle with index of refraction less than the surrounding medium, $n_1 < n_o$. (**d**) Trapping a low-index particle using a dark optical trap.

2. Far-field optical manipulation at the nanoscale

2.a. Single molecules and DNA.

Transparent high refractive index dielectric spheres of diameter $\approx$ 0.2 - 10 µm (polymer or silica) are typically used in optical trapping. The quantification of the position and force for each optical trapped microsphere offers a direct measurement of translation motion and

mechanical forces in biological or colloidal systems. Optical tweezers are able to manipulate macromolecules (kinesin or DNA) in an indirect fashion. Dielectric microspheres can be used as handlers of macromolecules labelled with biotin. Polystyrene microspheres can be coated with streptavidin, which binds to biotin with high affinity [40], thus enabling tethering between the macromolecule and the the microsphere. The microspheres function as physical "handles" facilitating indirect manipulation of the macromolecules. Block, *et al* did pioneering experiments to measure the steps taken by kinesin, a molecular porter [41]. During its motion along a fixed microtubule track created upon a microscope slide, the kinesin molecule moves along in a "jerky" stride with alternating step sizes. **Figure 3a** shows a microsphere bound with appropriate surface chemistry to a single kinesin molecule, as described earlier, and then held close to its microtubule track with an optical tweezers [42]. A buffered salt solution containing the chemical fuel adenosine triphosphate (ATP) constituted as the sample medium. The use of a single optical tweezers and a quadrant photodiode (QPD) permitted the detailed observations of the kinesin motor and microtubule track interaction. The trapped microsphere was pulled by the kinesin and the experiment was able to reveal approximately 8 nm steps taken by the kinesin molecule. The behaviour of the kinesin molecule was attributed to it pausing at random intervals, after taking each step as it waited for a fresh ATP molecule to arrive. Hence, studying motor proteins using an optically trapped microsphere enables better understanding the mechanics of single molecule [43-44]. In DNA studies, the ability to stretch DNA using optical forces can provide pertinent information on the elasticity of DNA strand much like a polymer fibre [45-47]. Optical trapping of microspheres has produced some seminal studies in single molecule biophysics and allowed breakthrough insights into mechanical properties of single molecules.

2.b. Metallic nanoparticles

When the size of the metallic or gold particle is brought down to around 100 nm, the optical forces that act upon the particles radically change. In principle, from Eq. 2, it is easy to infer that the gradient force in the Rayleigh regime is directly proportional to the polarizability, α, of the object. Gold nanoparticles possess a much larger polarizability than the dielectric particles of the same size (100 nm and below) [48]. The dielectric function of gold is a complex number ε_{Au} = -54 + i5.9 at λ=1.047um [10, 48], where ε is the material's relative permittivity, which is associated with the refractive index, $n = \sqrt{\varepsilon\mu}$, with μ is the relative permeability of the material at the optical frequency. Using a trapping light with wavelength that is further away from the resonance wavelength ($\lambda_{res}\approx$0.5um), the scattering and absorption coefficient is greatly reduced while the polarizability may remain unchanged. The polarizability, α, in Eq. 1, is derived from the Claussius-Mossotti relation:

$$\alpha_{Au} = V\left(\varepsilon_{Au} - \varepsilon_{H_2O}/\varepsilon_{Au} + 2\varepsilon_{H_2O}\right), \tag{3}$$

where V is the volume of the particle and ε_{H_2O} is the permittivity of water. The skin depth of gold is about 23 nm and for particles with radius smaller than the skin depth is considered uniformly polarized. Hence for particles with radius larger than the skin depth, the particle shape can influence the polarizability. From Eq. 2 it is likely that the strong reduction in the scattering forces and large enhancement of the polarizability of the gradient forces brings about stable optical trapping of gold nanoparticles in 3D.

Svoboda and Block were the first to demonstrate stably trapped single gold nanoparticles (36 nm in diameter) in 3D [10]. Whilst the particle is far smaller than the beam waist, the enhanced polarizability of gold as compared to the dielectric sphere creates a much stronger trapping strength. This pioneering work spawns the possibility of using optical forces to manipulate nanoparticles. The size of particles that is within the trapping range of a single

beam tweezers now extends towards tens of nanometres (i.e. semiconductor quantum dots) [49-50]. Apart from gold, trapping of other metallic particles such as platinum nanoparticles has also been demonstrated [51]. Metallic nanoparticles offer new phenomena to explore such as localised heating source. Dramatic heating has been observed in gold nanoparticle trapped with a focused infrared laser beam [52]. Seol *et al* studied the increase in temperature (ΔT) of a gold nanoparticle based on its absorbed optical power as follows, $\Delta T(r) = P_{abs}/4\pi\rho C$ where P_{abs} is the absorbed power, ρ is the radius of the sphere and C is the conductivity of the medium [52]. With this formula, they calculated a 266 ^{o}C/W based on a 50 nm (radius) gold nanoparticle with an illuminating near infrared beam (wavelength of 1064 nm, beam waist of 427 nm). Controlled *in vitro* cell hyperthermia using heated nanoparticles has numerous therapeutic purposes especially in the controlled destruction of cancerous cells. Metallic nanoparticle, with relatively high absorption co-efficient at a given optical wavelength, can create highly localised thermal bath [53]. Using this technique, a single optically trapped metallic gold nanoparticle can be used as a localized heating source [54, 55]. Optical trapping of airborne gold nanoparticles also results in heating associated with nanoparticle absorption of the trapping beam [55]. This effect has been exploited to achieve nanoscale cell hyperthermia [56].

2.c. Semiconductor quantum dots and nanowires.

The combination of far-field optical trapping with microfluidics as well as electrostatic interactions with an applied external electric field has been used to manipulate semiconductor nanostructures [57-64]. Compared with metallic nanoparticles, semiconductor 1D nanostructures (e.g ZnO, GaAs, Si) has a relatively high refractive index at the near infrared wavelength which is ideal for optical trapping. However, their overall aspect ratio (diameter to length of 1:20) still poses a substantial hurdle to their efficient manipulation [60-61]. An immediate solution would be to use multiple optical tweezers systems, e.g. holographic optical tweezers (discussed in the next section) or time-shared optical tweezers to tackle this concern. By distributing either a discrete number of optical tweezers or an elongated optical trap (a line intensity pattern) over the nanostructures, the 1D nanostructure is optically confined in either 2D or 3D[62]. In **figure 3b**, Van der Horst *et al* used an AOD to create multiple optical traps in a counter-propagating beam trapping geometry [63]. The nanowires are transported to the top of the sample and deposited onto two microspheres. Recent advancements in optoelectronic tweezers have also shown the ability to manipulate a large number of single nanowires simultaneously in 2D[64]. In addition, optical tweezers have shown to selectively transport and deposit bundles of single or multi walled carbon nanotubes onto a substrate [65-68]. The study of the interaction between light and an ensemble of nanoparticles can prove to be an important platform for nanophotonics *i.e.* building nanostructures from an ensemble of nanoparticles. Moreover, spectral measurements can be incorporated and measurement of spectral properties of optically trapped silicon nanoparticles with scattering properties exhibiting strong dielectric resonances provides a unique marker for probing size, shape, orientation and local dielectric environment [69].

2.c. Non-linear Kerr effects in optically trapped particles

Optical traps can initiate nonlinear optical responses in a colloidal mixture nanoparticles acting as artificial Kerr media [70-73]. Ashkin *et al* first demonstrated these nonlinear effects such as self-focusing/self-trapping (see **Fig. 3c**) [70-71], four-wave mixing [72] and optical bistability [73] in an ensemble of colloidal nanoparticles. These pioneering experimental demonstrations that use continuous wave (CW) lasers showed that the optical forces could induce a strong nonlinear response at relatively low average powers (~1-2W). In the presence of an optical field, nanoparticles experience an electrostrictive volume force (optical gradient forces) that attracts them into the spatial regions of high intensity, consequently increasing

the local density and the local refractive-index. Particles in an optical field can therefore act as an artificial Kerr media, where the induced change in refractive-index, Δn, is proportional to the applied light intensity I, $\Delta n = n_{2k}I$, where $n_{2k} > 0$ is the Kerr coefficient. However, just considering the dominant optical forces would result in a lead to an exponential variation of index change with intensity, $\Delta n = n_{2k}\exp\big((\alpha/4k_BT)I\big)$, where α is the polarizability of the particle, k_B is Boltzmann constant and T is temperature of the medium. Recently, both El-Ganainy *et al* [74] and Gordon *et al* [75] have suggested that the full exponential model should be employed to investigate the nonlinear responses in a colloidal suspension at low colloidal densities. However, including the full exponential model renders the nonlinear responses highly unstable. This is in apparent contradiction with recent experimental observations of relatively stable one-dimensional Kerr medium with evanescent fields that seem to agree reasonably with the Kerr model [76]. To resolve this issue, Matuszewski *et. al* have shown that by treating the nanosuspension as a hard sphere gas, it is possible to include the compressibility of the system, which explains the saturation of the exponential nonlinearity at high intensities [77]. The inclusion of the particle compressibility with experimental parameters marked an important step towards resolving which theoretical model best describes the phenomenon. This has been shown experimentally using a dual beam fiber z-scan approach as shown in **Figure 3d**[78]. Including the effects of compressibility via the second virial coefficient in the non-ideal gas model was found to yield good agreement with the experiment, and in turn can be used to infer values for the second virial coefficient and the nonlinear coefficients.
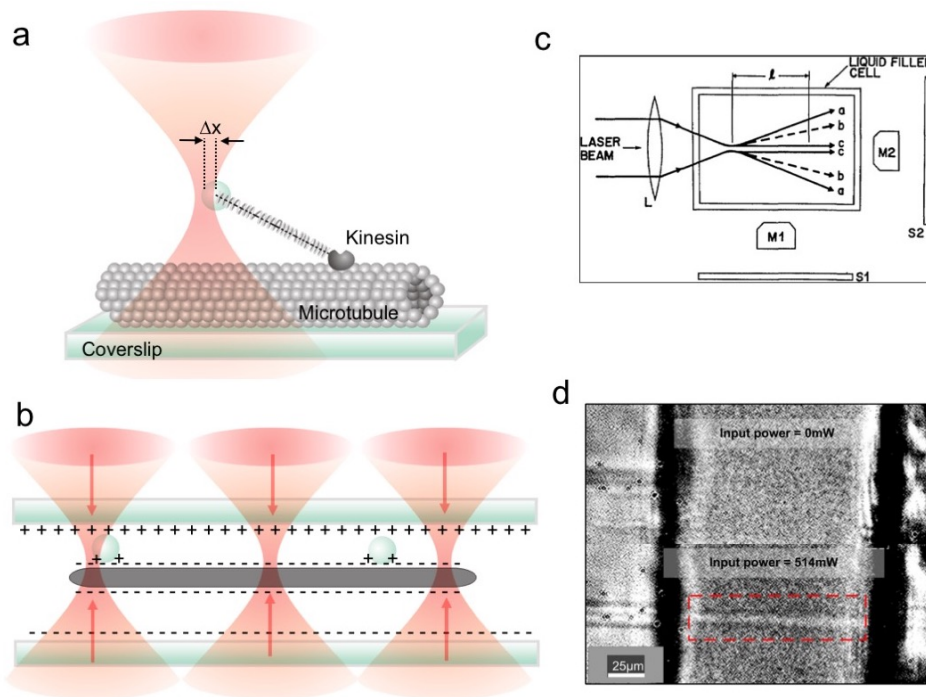

Figure 3. (a) The diagram illustrates an optical force clamp recording displacements of single kinesin molecules while maintaining an average load. **(b)** A sketch showing a Zinc oxide (ZnO) nanowire trapped in counter-propagating optical traps. Optical traps transport the nanowires to the top surface of the cell enabling silica particles coated with PAH to give them a positive charge to be deposited onto the nanowire. When pressed against the top surface the nanowire will stick via electrostatic interactions. Here the nanowire is shown to form a bridge between two spheres [63]. **(c)** Self-focusing and self-trapping experiment performed by Ashkin, et al [70]. ©Optical Society of America. **(d)** DIC image of the edge of two fibers (input on the left and collected on the right) in the nanosuspension. The top image indicates no accumulation (*P*=0 mW), while the bottom image shows a fine channel of accumulating nanoparticles (red box) at *P*=514 mW[78]. ©Optical Society of America. *(Permission to reuse the images will be acquired from relevant sources).*

3. Extending far-field optical trapping with structured light

To achieve optimal optical trapping conditions for a range of particles, the trapping light need not be a single focused light. The trapping laser can be tailored to suit the optical properties of the particles to be trapped. A key ingredient to produce structured optical traps and effectively transfer photon momentum is to project light patterns from a single laser with high optical throughput. This can be achieved by modulating the wavefront of the incident light, using a phase-only spatial light modulator (SLM). The phase-encoded light is optically transformed to project the desired spatial patterns at the output. To achieve a full-complex field holographic projection[79], we combine two techniques: (1) Generalized Phase Contrast (GPC) method [25-26,80-82]; and (2) phase-only holographic method[30-34]. Let us briefly discuss these methods separately and work towards achieving an optimal light projection technique suitable for generating structured beam optical traps.

3.a. Holographic projection

Figure 4 shows different modalities to achieve far-field structured light illumination for optical traps. **Figure 4a** shows the holographic projection method, which entails the pre-calculation of a computer-generated hologram (CGH) and encoding it on either a diffractive optical element [29] or spatial light modulator [30-32]. When the hologram is illuminated, the optical transformation in the far field (or at the focus of a lens) projects the arbitrary optical field patterns. Calculation of the CGH can be achieved via an iterative optimization algorithm or by the superposition of combined prism and lens phase functions to independently position each trapping beam [30-32]. The 3D intensity distribution of the holographically projected multiple foci is shown in **Fig. 4b**, which is characterized by the convolution of N delta functions and the Fourier transform of a circular aperture associated with the 3D point-spread function of the optical system. As such, the circularly symmetric two-dimensional (2D) intensity profile of each diffraction-limited spot is described by the normalized Airy pattern.

3.b. Generalized Phase Contrast Method

The GPC method, on the other hand, is an imaging approach where the phase pattern encoded at the SLM is an exact representation of the intensity pattern projected at the output. The GPC method is basically a common path interferometer [81], where a phase-shifted component of the incident light interferes with an unperturbed component. **Figure 4c** shows the schematic of the GPC method showing a 4f lens configuration with a phase-shifted zero-order component (focus light at the Fourier plane). The spatial phase-only filter or phase-contrast filter (PCF) at the Fourier plane converts a phase pattern into a high-contrast intensity image. The first lens performs a spatial Fourier transform setting up the low frequency component of the input laser to focus onto the central filtering region of the PCF which sets the focus to be shifted by π. On the other hand, high frequency components get scattered outside the filtering region. With the low frequency component phase-shifted by π, its interference with the high frequency components converts the phase pattern at the input to a high-contrast intensity pattern after the second lens performs an inverse Fourier transform. The phase of the PCF, however, can be modified for complex projection of greyscale patterns [83] or can be designed with a ring to improve the uniformity of the intensity distribution [84].

3.c. Full complex field holographic projection

The use of phase-only devices in holographic projection results in the projection of unnecessary spurious orders at the output. Intricate output patterns will require encoding of a complex field at the input and truncating the input function to use a phase-only SLM results in projection of unwanted high diffraction orders [85]. Simply applying an amplitude spatial light modulator in addition to a phase-only device to represent a full complex field reduces

the light throughput significantly. To improve the optical throughput, the GPC method can be used to generate the necessary amplitude modulation at the hologram plane. **Figure 4e** shows the principle and geometry of full complex holographic projection using a combination of GPC and holographic projection [79]. To efficiently generate patterns at the output, the field at the hologram plane should contain both amplitude and phase functions. The appropriate amplitude and phase functions to produce a particular pattern can be calculated via wave theory. The left side of **Figure 4e** shows the GPC method, where the amplitude is mapped out as a phase pattern and encoded unto a phase-only SLM.
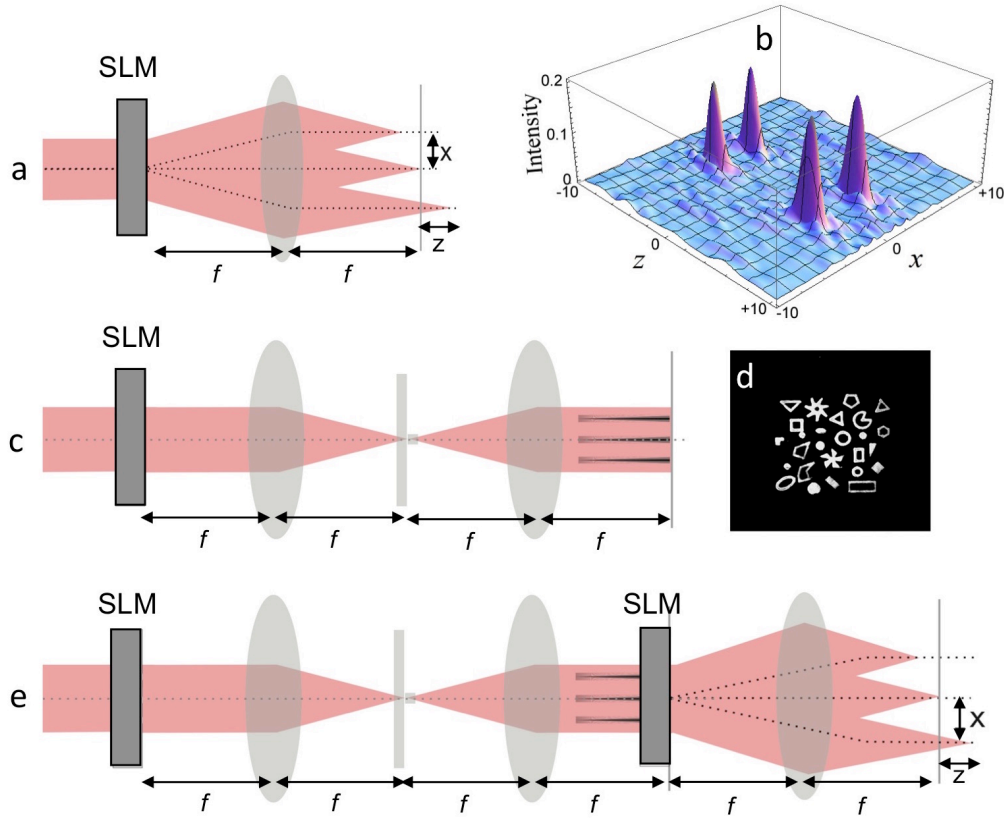

Figure 4. Optical approaches to produce far-field structured light illumination. (**a**) Phase-only holographic projection. (**b**) Numerically evaluated intensity distribution of four spots along the *xz*-plane. (**c**) Generalized Phase Contrast method that converts an input phase into high-intensity pattern suitable for multiple optical traps. (**d**) Sample output intensity pattern showing various light patterns for various trapping configurations. (**e**) Full complex field holographic projection using an amplitude pattern generated via the Generalized Phase Contrast method [79].

3.d Optical trapping with structured light

Using structured beams as multiple beam optical traps facilitate manipulation of particles with different optical properties. Tailoring of the profile and parameters of an optical field provide optimal conditions for effective use of light's momentum. In the same way, tailored optical fields that split up a single laser into multiple trapping potentials open up opportunities for studying multiple particle interactions. **Figure 5a** shows pioneering demonstration of particles trapped in a fixed 4×4 holographic optical trap array by Drufresne, *et al* [29]. Using a spatial light modulator, Curtis, *et al* demonstrated dynamically reconfigurable optical traps as shown in **Fig. 5b**[32]. **Figure 5c** shows the first 2 frames (0.24s apart) for real-time dynamic manipulation of multiple particles trapped via the GPC method[35]. The particles in the outer ring rotates clockwise while the particles in the inner

ring rotates counter clockwise. Rotation is achieved via the transfer of linear momentum with optical traps manipulated directly via the phase-contrast projection of a phase pattern encoded from the computer. **Figure 5d** shows 3D optical traps, which can be dynamically reconfigured in real-time enabling four-dimensional (4D) optical manipulation [86]. **Figure 5e** and **5f** shows simultaneous transfer of linear momentum and OAM in a holographic projection setup producing both Gaussian and Laguerre-Gaussian optical traps with helical wavefront [28]. In **Fig. 5f**, the two particles revolve around the doughnut beam via transfer of (OAM) with opposite chirality, while the doughnut beams are translated to rotate clockwise.
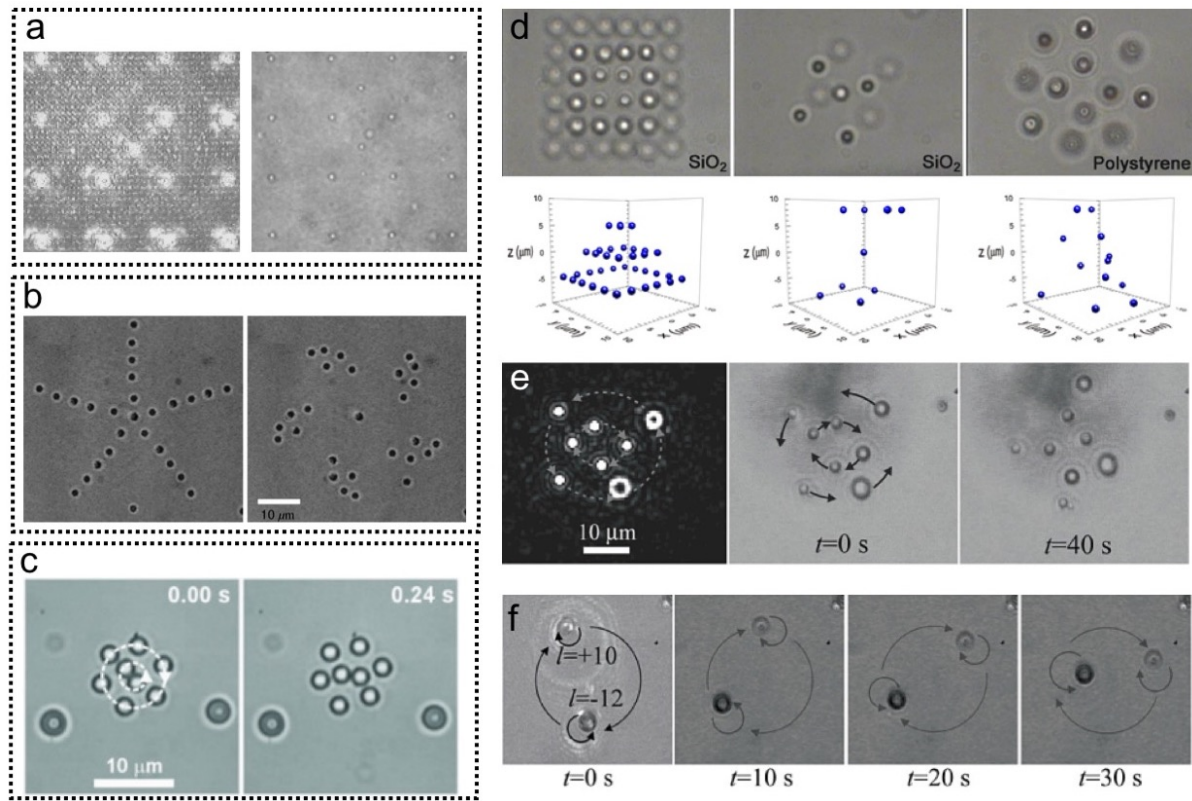

Figure 5. (**a**) Pioneering demonstration of a fixed 4×4 holographic optical trap (left) with optically trapped particles (right) by Drufresne and Grier [29]. ©American Institute of Physics. (**b**) Dynamic holographic optical tweezers using a computer programmable SLM [32]. ©Elsevier, Inc. (**c**) The first two frames of the video showing real-time micromanipulation of multiple particles using the GPC method [35]. Video of the experiment can be downloaded from Eriksen, *et al*. [35]. ©Optical Society of America. (**d**) Four-dimensional (3D+real-time) micromanipulation of multiple particles using the GPC method [86]. ©American Physical Society. (**e**) & (**f**) Simultaneous transfer of linear momentum and OAM using holographic projection of multiple Gaussian and Laguerre-Gaussian beams [28]. In (**f**), two particles rotate along the ring-shaped doughnut beam with opposite chirality. The doughnut beams are also moved clockwise along a circular orbit. ©Institute of Optics. *(Permission to reuse the images will be acquired from relevant sources).*

3.e. Manipulation of plasmonic nanostructures with structured light

Far field optical traps with structured beams have been used to perform trapping of plasmonic nanostructures, such as metal nanoparticles and nanorods. Dienerowitz *et al* has experimentally demonstrated optical trapping near the plasmon resonance using an optical vortex possessing a helical wavefront [87]. The nanoparticles are confined in the vortex core (dark) region and rotate due to the transfer of orbital angular momentum. Theoretical

investigations to excite multipole plasmons in metal nanodisks can be selectively excited by circularly-polarized optical vortex beams [88]. Sakai *et al* argues that dark mode plasmons circumvent radiation loss and store the energy longer [88]. Plasmonic nanowires have been optically trapped in 3D using an extended trapping-beam with depth-of-focus derived from the Fourier transform of a linearly polarized Bessel beam [89]. The extended depth of focus enables the use of a retroreflection geometry to cancel radiation pressure in the beam propagation direction, making it possible to trap highly scattering and absorbing silver nanowires. Yan *et al*, also showed trapping of multiple nanowires simultaneously in spatially separated maxima of the trapping beam[89].

4. Near-field optical manipulation
4.a. Manipulation by evanescent waves

The transfer of optical momentum with evanescent fields started with pioneering experiments by Kawata and Sugiura [90]. **Figure 6a** shows the schematic of the transfer of linear momentum from an evanescent field produced at the interface between two media with indices of refraction, n_1 and n_2. This work led to theoretical predictions using sharp metallic tips to create an optical trap that can trap dielectric objects as small as a few tens of nanometers[91-94]. Novotny, *et al* worked on a numerical model of the near field at gold tip. **Fig. 6b** shows their numerically calculated contours of the near field (E^2) at the gold tip immersed in water when illuminated by a monochromatic wave (λ=810 nm) that does not excite surface plasmons. **Figure 6b(left)** shows illumination from the bottom while **Fig. 6b(right)** shows illumination from the side[93]. On the other hand, Okamoto and Kawata proposed an optical trap using the light transmitted through a nano-aperture in an opaque metallic film [95]. In either case, the illuminated nanostructure/nanoaperture functions as a lens that produced a focused near-field optical trap capable of inducing the gradient forces for optical trapping. Generating an optical potential from nanostructures/nano-aperture facilitates the formation of an array of near-field optical traps from a single beam enabling parallel trapping of multiple nanoparticles on a surface [96]. The near-field profile on surfaces will depend on the organization of nanostructures on the surface. To map out the profile of evanescent fields, Pin *et al* proposed to measure the thermal motion of fluorescent microbeads trapped in the near-field of silicon nanocavities [97].

Apart from the near-field produced in nanostructures and nano-apertures, manipulation by evanescent fields also paved way to using channel waveguides to manipulate dielectric microparticles [98] and gold Rayleigh particles [99]. Evanescent fields on planar integrated waveguides induce microparticles and biological cells to move on the waveguide surface via transfer of linear momentum [100-102]. Moreover, patterned evanescent waves formed from counter-propagating beams enabled the organization of microparticles on a surface over an extended area [103]. Particle sorting can also be achieved with two counter-propagating evanescent waves targeting plasmon resonances of gold nanoparticles of varying geometry [104].

4.b. Surface plasmon optical tweezers

Nanofabricated structures on substrates can provide enhanced surface fields where nanoparticles with known polarizability can be efficiently trapped[105]. Optical forces acting on metallic nanoparticles are substantially enhanced when they are trapped at a wavelength tuned to its plasmon resonance, as determined by the particles' geometry. The F_s for nanoparticles are relatively weak due to their size. However, excitation of surface plasmon polaritons assisted with thermal gradients can attract particles to self-assemble into colloidal aggregations [106, 107]. Aside from metallic nanoparticles, the motion of the dielectric particles on the metal surfaces can be attributed to radiation forces from the surface plasmon,

which facilitates the transfer of linear momentum to the dielectric particles [108]. The plasmon radiation force is measured to be dependent on the distance of the particle with respect to the metal surface.

To dynamically manipulate nanoparticles along the surface of metallic substrates, far field projection of structured light can be used to change focal regions of surface plasmons excited on metal surfaces. As shown in **Fig. 6c**, Huft *et al* [110] demonstrated a plasmonic hologram, which is obtained by illuminating structured light onto the perimeter of a silver Bull's Eye nanostructure to generate a focal point of surface plasmons towards the center. The location of the plasmon focus can be controlled by shifting the phase of the plasmon waves as a function of space, which in turn changes the location of the focal points and enable movement of particles trapped by the surface plasmon. Using a relatively similar nanostructure (spiral instead of concentric circles), Tsai *et al* has used a gold plasmonic Archimedes spiral structure to induce orbital rotation in a linear assembly of microparticles [111]. The direction of rotation depends on the handedness of the applied circularly polarized light to excite plasmonic near fields onto the Archimedes spiral. Similarly, rotation of single-crystal gold nanorods in aqueous solutions through optical torques can be achieved by plasmonic resonant scattering of circularly polarized laser light [112]. Moreover, using the trapping light's polarization, the induced surface plasmons on gold nanodiscs can make the discs rotate around a gold nanopillar [113]. The induced surface plasmons on nanopillars sets a gradient trap and depending on the chirality of the input circularly-polarized light, the microparticles showed selective particle trapping directed towards the spiral origin by a focusing spot or particle rotation along the primary ring caused by a plasmonic field. More recently, theoretical work proposes the use of vortex beams to induce dynamic steering of the surface plasmon focus, which can have potential for dynamic manipulation nanoparticles in a plasmonic tweezers [114].

Using a radially polarized beam to induce surface plasmons, metallic particles are attracted and trapped by plasmonic tweezers. The work by Min *et al*, proposes that trapping with plasmonic tweezers is not due to the balance between F_g and an opposing F_s, but results from the sum of both F_s and F_g acting in the same direction established by the strong coupling between the metallic particle and a highly focused plasmonic field [115]. Wang *et al* further showed that surface plasmon polaritons excited on gold nanoparticles coupled with the near-field on the film substrate results in enhanced optical forces enabling propulsion of the nanoparticles[116].

4.c. Plasmonic lattices

Surface plasmons excited within a standing wave optical trap can confine nanoparticles in the absence of thermal effects. The coherent superposition between the standing wave of the standing wave and the surface plasmon near field facilitates formation of gradient forces that influence particle motion [117]. Optical forces associated with negative refractive index have also been demonstrated by a plasmonic lattice with an equivalent structure as a photonic crystal. Cuche *et al*, demonstrated that periodically patterned metal film can produce a plasmonic lattice with periodically modulated near-field optical forces [118]. The plasmonic lattice is associated with negatively refracted surface plasmons, which can control particle trajectories similar to particle motions in a photonic lattice. **Figure 6d** graphically illustrates the particle trajectories through the plasmonic lattice. In a related work, transport, guiding and arrangement of nanoparticles has been demonstrated in a plasmon-enhanced two-dimensional plasmon-enhanced optical lattice consisting of a periodic array of gold nanostructures and illuminated by a Gaussian beam[119].
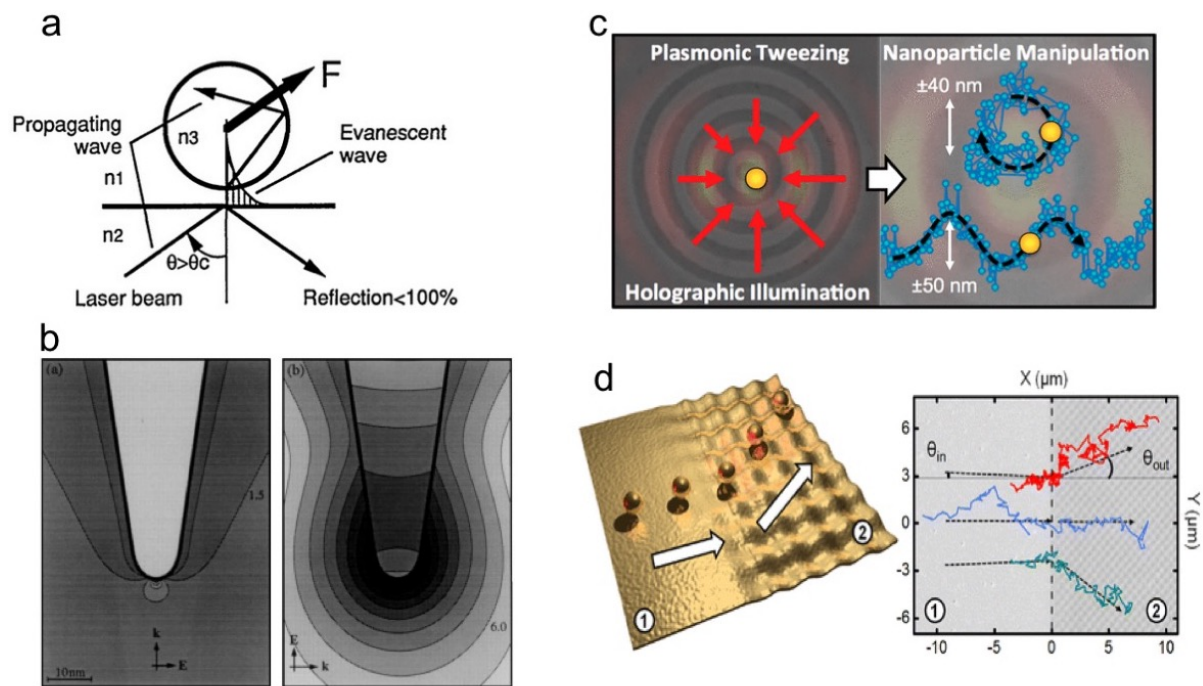
Figure 6. (**a**) Schematic showing the transfer of linear momentum from an evanescent field produced at the interface between two media with indices of refraction, n_1 and n_2. This pioneering experiment by Kawata, *et al* [90] led to near field optical traps. ©Optical Society of America. (**b**) Numerical model showing contours of the near field (E^2) of a gold tip in water illuminated by a monochromatic wave (λ=810 nm) that does not excite surface plasmons. The left figure shows illumination from the bottom while right figure shows illumination from the side[93]. ©American Physical Society. (**c**) A computer-generated hologram produces structured beam to illuminate the perimeter of a silver substrate with a Bull's eye nanostructure. The nanostructure generates surface plasmons that propagate and focus towards the center. The position of the surface plasmon focus can be controlled by changing the hologram, thereby manipulating nanoparticles trapped at the plasmon focus [110]. ©American Chemical Society. (**d**) Near-field optical forces from a periodically patterned metal film depicts that of a plasmonic lattice with negatively refracted surface plasmons for controlling particle trajectories [118]. ©American Chemical Society. *(Permission to reuse the images will be acquired from relevant sources).*

5. Summary and future outlook

For nearly 50 years, optical manipulation has revolutionized various fields of science and providing us with a powerful tool to understand various phenomena from atoms, molecules to cells. We have briefly summarised various topics in optical trapping starting with far-field manipulation of single molecules to nanoparticle ensembles exhibiting nonlinear Kerr effects. Apart from single optical traps, we also discussed ways to obtain structured light for parallel optical manipulation of multiple particles. Although far-field optical traps can manipulate particles much smaller than the focus, more accurate manipulation of nanoparticles can be achieved in the near-field regime. Pioneering works on trapping via evanescent waves on surfaces and metallic tips paved way to manipulate particles that are smaller than the diffraction limit. Apart from evanescent waves, nanoparticles can be manipulated by surface plasmon polaritons on metallic surfaces ranging from flat to periodic structures that form plasmonic lattices.

While optical manipulation was initially applied to understand atomic, molecular and protein dynamics, its implications to more complex biological structures such as cells and organelles remain promising future directions [120]. Although direct laser illumination of

cells can provide direct heating and even surgery of cells [121,122], the combination of manipulation and plasmonic excitation on nanoparticles can provide a more accurate manipulation of proteins and cells beyond the diffraction limit[54-56]. Single myosin can be activated by heat via optically trapped gold nanoparticles [125].   Exciting surface plasmons on gold nanoparticles have been used to excite membranes of cells. This heat increases the local membrane temperature and consequently changes the membrane capacitance thereby inducing depolarization and action potentials in neurons [126,127]. Gold nanorods deposited in close proximity to membranes of cultured neurons [128,129] and to dendrites *in vivo*[130] have been shown to excite neurons when the laser is incident on the nanorods. New biocompatible nanoparticles that bind to the cellular membrane, such as ligand-conjugated gold nanoparticles, have been developed [131]. Structured light has also been used to excite multiple locations around the cell via thermal stimulation [132]. Localized heating triggers the opening of temperature-sensitive transient receptor potential vanilloid (TRPV) ion channels, which causes the cells (particularly neurons) to depolarize [133].

Optical manipulation has also been demonstrated to guide the growth of dendrites and axons in neurons as well as aid in the formation of dendritic spines. Weak optical forces have been initially shown to guide the direction of a growth cone of a nerve cell using a focused near-IR laser (800 nm) spot placed in front of a nerve's leading edge [134]. Gradient forces bias the actin polymerization and drive the extension of the lamellipodia, which is a cytoskeletal protein actin projection. Intracellular organelles can also be manipulated [122] and tracked [123,124] by optical forces with nanoscale accuracy. Optical manipulation of cytoplasmic structures in neurons could provide fundamental understanding of synaptic transmission and protein transport within the cell. Hosokawa, *et al.* [135] demonstrated optical manipulation of synaptic vesicles ($\rho \sim 20$ nm) providing artificial control of synaptic transmission in a neuronal network. On the other hand, Chowdary, *et al.* [136] made use of nanoparticles to tether endosomes making it possible to study the cooperative mechanics of dyneins on retrograde axonal endosomes in live neurons. Dynein is a motor protein that drives the transport of various cellular cargos from the different regions of the neuron to the soma and is therefore vital for its function.

So far, optical manipulation of cells, organelles and vesicles has been implemented in artificial cellular environments or *in vitro* preparations (*e.g.* cell cultures). The future points to applying optical manipulation in an intact living animal (*in vivo*) to answer unresolved neurobiological questions. Understanding the cascade of events starting from a biomolecular stimulus to neuronal circuit processing and leading to the animal's behavioural response remains a challenge. Recently, *in vivo* optical traps enabled the manipulation of otoliths (or ear stones) in a living larval zebrafish to trigger fictive vestibular stimuli whilst the fish is stationary [137]. Applying optical forces on the otoliths results in tail movements and sufficient to cause a rolling correction in the fish's eyes. Such controlled manipulation of the vestibular system enables a systematic study of neuronal circuit processing that explains how animals detect gravity and motion. Future experiments involving *in vivo* optical manipulation combined with functional imaging of cellular activity are likely to provide ways to understand basic neuronal processes that trigger animal behaviour. While *in vivo* optical manipulation of red blood cells has been demonstrated in more complex animals with turbid tissues [138], highly targeted optical nanomanipulation of subcellular organelles/proteins or embedded nanoparticles in semi-transparent animals (e.g. zebrafish) can aid in our understanding of the basic cellular and biomolecular mechanisms that stimulates behavioural responses. A recent study on the uptake of gold plasmonic nanoparticle in a developing zebrafish embryo has shown that particles ~100nm in diameter are more biocompatible than smaller ones (~10nm) [139]. Other metallic nanoparticles (e.g. Ag, CuO and ZnO) have also

been tested for biocompatibility (or conversely toxicity) [140,141]. Hence, using optical traps to manipulate minute mechanical movements and/or excite surface plasmons on metallic nanoparticles taken up by living animals will provide a more targeted technique to probe fundamental cellular activity.

These exciting future applications prove optical manipulation to be a significant tool that will continue to evolve to complement the complexities and challenges of novel and unresolved research problems. The broad range of applications (from atoms, molecules, cells to whole organs in complex animals) and covering a wide scale (from nanometers to micrometers) makes optical manipulation a truly revolutionary tool worthy of commendation.

Acknowledgements

References

1. A. Ashkin, Acceleration and trapping of particles by radiation pressure, *Physical Review Letters* **24**, 156-159 (1970).
2. A. Ashkin, Optical trapping and manipulation of neutral particles using lasers, *Proc of the Natl Acad of Sci USA* **94**, 4853 - 4860 (1997).
3. A. Ashkin, J. M. Dziedzic, J. E. Bjorkholm, and S. Chu, Observation of a single-beam gradient force optical trap for dielectric particles, *Optics Letters* **11**, 288-290 (1986).
4. C. N. Cohen-Tannoudji, Manipulating atoms with photons, *Reviews of Modern Physics* **70**, 707-719 (1998).
5. W. D. Phillips, Laser cooling and trapping of neutral atoms, *Reviews of Modern Physics* **70**, 721-741 (1998).
6. M. R. Andrews, C. G. Townsend, H. J. Miesner, D. S. Durfee, D. M. Kurn, and W. Ketterle, Observation of interference between two Bose condensates, *Science* **275**, 637-641 (1997).
7. K. B. Davis, M. O. Mewes, M. R. Andrews, N. J. Vandruten, D. S. Durfee, D. M. Kurn, and W. Ketterle, Bose-Einstein condensation in a gas of sodium atoms, *Physical Review Letters* **75**, 3969-3973 (1995).
8. A. Ashkin, Forces of a single-beam gradient laser trap on a dielectric sphere in the ray optics regime, *Biophysical Journal* **61**, 569-582 (1992).
9. Y. Harada, and T. Asakura, Radiation forces on a dielectric sphere in the Rayleigh scattering regime, *Optics Communications* **124**, 529-541 (1996).
10. K. Svoboda, and S. M. Block, Optical Trapping of Metallic Rayleigh Particles, *Optics Letters* **19**, 930-932 (1994).
11. A. Ashkin, History of optical trapping and manipulation of small-neutral particle, atoms, and molecules, *IEEE Journal of Selected Topics in Quantum Electronics* **6**, 841-856 (2000).
12. K. C. Neuman, and S. M. Block, Optical trapping, *Review of Scientific Instruments* **75**, 2787-2809 (2004).
13. J. A. Lock, Calculation of the Radiation Trapping Force for Laser Tweezers by Use of Generalized Lorenz-Mie Theory. I. Localized Model Description of an On-Axis Tightly Focused Laser Beam with Spherical Aberration, *Applied Optics* **43**, 2532-2544 (2004).
14. J. A. Lock, Calculation of the Radiation Trapping Force for Laser Tweezers by Use of Generalized Lorenz-Mie Theory. II. On-Axis Trapping Force, *Applied Optics* **43**, 2545-2554 (2004).
15. A. A. R. Neves, A. Fontes, L. d. Y. Pozzo, A. A. de Thomaz, E. Chillce, E. Rodriguez, L. C. Barbosa, and C. L. Cesar, Electromagnetic forces for an arbitrary optical trapping of a spherical dielectric, *Opt. Express* **14**, 13101-13106 (2006).
16. J. P. Barton, and D. R. Alexander, Fifth-order corrected electromagnetic field components for a fundamental Gaussian beam, *Journal of Applied Physics* **66**, 2800-2802 (1989).
17. J. P. Barton, D. R. Alexander, and S. A. Schaub, Theoretical Determination of Net-Radiation Force and Torque for a Spherical-Particle Illuminated by a Focused Laser-Beam, *Journal of Applied Physics* **66**, 4594-4602 (1989).

18. A. Rohrbach, and E. H. K. Stelzer, Trapping forces, force constants, and potential depths for dielectric spheres in the presence of spherical aberrations, *Applied Optics* **41**, 2494-2507 (2002).

19. A. Rohrbach, Stiffness of optical traps: Quantitative agreement between experiment and electromagnetic theory, *Physical Review Letters* **95**, 168102 (2005).

20. H. He, N.R. Heckenberg, H. Rubinsztein-Dunlop, Optical particle trapping with higher-order doughnut beams produced using high efficiency computer generated holograms, *Journal of Modern Optics* **42**, 217 (1995).

21. N.B. Simpson, L. Allen, M.J. Padgett, Optical tweezers and optical spanners with Laguerre-Gaussian modes, *Journal of Modern Optics* **43**, 2485–2491 (1996).

22. K.T. Gahagan, G.A. Swartzlander, Optical vortex trapping of particles, *Optics Letters* **21**, 827–829 (1996).

23. K.T. Gahagan, G.A. Swartzlander, Trapping of low-index microparticles in an optical vortex, *Journal of the Optical Society of America B* **15**, 524-534 (1998)

24. K.T. Gahagan, G.A. Swartzlander, Simultaneous trapping of low-index and high-index microparticles observed with an optical-vortex trap, *Journal of the Optical Society of America B* **16**, 533-537 (1999).

25. V.R. Daria, P.J. Rodrigo, J. Glückstad, Dynamic array of dark optical traps, *Applied Physics Letters* **84**, 323-325 (2004)

26. P.J. Rodrigo, V.R. Daria, J. Glückstad, Real-time interactive optical micromanipulation of a mixture of high- and low-index particles, *Optics Express* **12**, 1417-1425 (2004)

27. H. Furukawa, and I. Yamaguchi, Optical trapping of metallic particles by a fixed Gaussian beam, *Optics Letters* **23**, 216-218 (1998).

28. V.R. Daria, M.A. Go, H.A. Bachor, Simultaneous transfer of linear and orbital angular momentum to multiple low-index particles, *Journal of Optics* **13**, p044004 (2011).

29. E. Drufresne and D. G. Grier, Optical tweezer arrays and optical substrates created with diffractive optics, *Review of Scientific Instruments* **69**, 1974 (1998).

30. J. Liesener, M. Reichester, T. Haist, and H.J. Tiziani, Multi-functional optical tweezers using computer generated holograms, *Optics Communications* **185**, 77-82, (2000).

31. E. R. Dufresne, G. C. Spalding, M. T. Dearing, S. A. Sheets, and D. G. Grier, Computer-generated holographic optical tweezer arrays, *Rev. Sci. Instrum.* **72**, 1810, (2001).

32. J.E. Curtis, A. Koss, D.G. Grier, Dynamic holographic optical tweezers, *Optics Communications* **207**, 169-175, (2002).

33. K. Ladavac and D.G. Grier, Microoptomechanical pump assembled and driven by holographic optical vortex arrays, *Optics Express* **12**, 1144-1149 (2004)

34. P. Prentice, M. MacDonald, T. Frank, A. Cuschier, G. Spalding, W. Sibbett, P. Campbell, and K. Dholakia, Manipulation and filtration of low-index particles with holographic Laguerre-Gaussian optical trap array, *Optics Express* **12**, 593-600, 2004.

35. R. L. Eriksen, V.R. Daria and J. Gluckstad, Fully dynamic multiple-beam optical tweezers, *Optics Express* **10**, 597-603, 2002.

36. H. He, M.E.J. Friese, N.R. Heckenberg, H. Rubinsztein-Dunlop, Direct observation of transfer of angular momentum to absorptive particles from a laser beam with a phase singularity *Physical Review Letters* **75,** 826-829 (1995).

37. M.E. J. Friese, H. Rubinsztein-Dunlop, J. Enger, N.R. Heckenberg, Optical angular momentum transfer to trapped absorbing particles, *Physical Review A* **54,** 1593-1596 (1996)

38. V. Garces-Chavez, K. Volke-Sepulveda, S. Chavez-Cerda, W. Sibbett, K. Dholakia, Transfer of orbital angular momentum to an optically trapped low-index particle, *Physical Review A* **66,** 063402 (2002)

39. L. Allen, M. Beijersbergen, R. Spreeuw, J. Woerdmann, Orbital angular momentum of light and the transformation of Laguerre-Gaussian laser modes, *Physical Review* **A** 45 8185 (1992).

40. D.C. Appleyard, *et al.*, Optical trapping for undergraduates*, American Journal of Physics* **75,** 5-14 (2007).

41. S.M. Block, L.S.B. Goldstein, and B.J. Schnapp, Bead Movement by Single Kinesin Molecules Studied with Optical Tweezers*, Nature* **348,** 348-352 (1990).

42. K. Visscher, M.J. Schnitzer and S.M. Block, *Single kinesin molecules studied with a molecular force clamp.* Nature **400**, 184-189 (1999).

43. W.J. Greenleaf, M.T. Woodside, and S.M. Block, High-resolution, single-molecule measurements of biomolecular motion, *Annual Review of Biophysics and Biomolecular Structure* **36**, 171-190 (2007).

44. A.D. Mehta, *et al.*, Single-molecule biomechanics with optical methods. *Science* **283,** 1689-1695 (1999).

45. T.T. Perkins, *et al.*, Relaxation of a Single DNA Molecule Observed by Optical Microscopy, *Science* **264,** 822-826 (1994).

46. S.B. Smith, Y.J. Cui, and C. Bustamante, Optical-trap force transducer that operates by direct measurement of light momentum, *Methods in Enzymology* **361**, 134-162 (2003).
47. C. Bustamante, Z. Bryant, and S.B. Smith, Ten years of tension: single-molecule DNA mechanics, *Nature* **421,** 423-427 (2003).
48. P. M. Hansen, V. K. Bhatia, N. Harrit, and L. Oddershede, Expanding the optical trapping range of gold nanoparticles, *NanoLetters* **5**, 1937-1942 (2005).
49. K.C. Neuman and S.M. Block, Optical trapping, *Review of Scientific Instruments* **75**, 2787-2809 (2004).
50. K. Dholakia and P. Reece, Optical micromanipulation takes hold, *Nano Today* **1**, 18-27 (2006).
51. A. Samadi, P. M. Bendix, L.B. Oddershede, Optical manipulation of individual strongly absorbing platinum nanoparticles, *Nanoscale* **9**, 18449-18455 (2017).
52. Y. Seol, A.E. Carpenter and T.T. Perkins, Gold nanoparticles: enhanced optical trapping and sensitivity coupled with significant heating, *Optics Letters* **31**, 2429-2431 (2006).
53. X. Huang, *et al*., Plasmonic photothermal therapy (PPTT) using gold nanoparticles. *Lasers in Medical Science* **23**, 217-228 (2008).
54. P.M. Bendix, S. Nader, S. Reihani and L.B. Oddershede, Direct measurement of heating by optically trapped gold nanoparticles using molecular sorting in lipid bilayers, *Biophysical Journal* **98**, 185 (2010).
55. L. Jauffred, *et al*, Optical trapping of gold nanoparticles in air, *Nano Letters* **15**, 4713-4719 (2015).
56. G.S. Terentyuk, *et al*., Laser-induced tissue hyperthermia mediated by gold nanoparticles: toward cancer phototherapy*, Journal of Biomedical Optics* **14**, 21016-9 (2009).
57. L. Jauffred, A.C. Richardson, and L.B. Oddershede, Three-Dimensional Optical Control of Individual Quantum Dots, *Nano Letters* **8**, 3376-3380 (2008).
58. T. Iida and H. Ishihara, Nano-optical manipulation using resonant radiation force, In: Ohtsu M. (Eds) *Progress in Nano-Electro-Optics VI*, *Springer Series in Optical Science* **139**, Springer, Berlin, Heidelberg (2008).
59. T. Yu, F.C. Cheong, and C.H. Sow, The manipulation and assembly of CuO nanorods with line optical tweezers, *Nanotechnology* **15**, 1732-1736 (2004).
60. P.J. Pauzauskie, *et al*., Optical trapping and integration of semiconductor nanowire assemblies in water, *Nature Materials* **5**, 97-101(2006).
61. Y. Nakayama, *et al*., Tunable nanowire nonlinear optical probe, *Nature* **447**, 1098-1101 (2007).
62. R. Agarwal, *et al*., Manipulation and assembly of nanowires with holographic optical traps, *Optics Express* **13**, 8906-8912(2005).
63. A. van der Horst, *et al*., Manipulating metal-oxide nanowires using counter-propagating optical line tweezers, *Optics Express* **15**, 11629-11639 (2007).
64. Y. Cui and C.M. Lieber, Functional nanoscale electronic devices assembled using silicon nanowire building blocks, *Science* **291**, 851-853 (2001).
65. D.L. Andrews and D.S. Bradshaw, Laser-induced forces between carbon nanotubes, *Optics Letters* **30**, 783-785 (2005).
66. L.F. Zheng, *et al*., Manipulating nanoparticles in solution with electrically contacted nanotubes using dielectrophoresis, *Langmuir* **20**, 8612-8619 (2004).
67. S.D. Tan, *et al*., Optical trapping of single-walled carbon nanotubes, *Nano Letters* **4**, 1415-1419 (2004).
68. J. Plewa, *et al*., Processing carbon nanotubes with holographic optical tweezers, *Optics Express* **12**, 1978-1981 (2004).
69. A. Andres-Arroyo, B. Gupta, F. Wang, J. J. Gooding and P.J. Reece, Optical manipulation and spectroscopy of silicon nanoparticles exhibiting dielectric resonances, *Nano Letters* **16**, 1903-1910 (2016).
70. A. Ashkin, J.M. Dziedzic and P.W. Smith, Continuous-wave self-focusing and self-trapping of light in artificial Kerr media, *Optics Letters* **7**, 276-278 (1982).
71. P.W. Smith, P.J. Maloney and A. Ashkin, Use of a liquid suspension of dielectric spheres as an artificial Kerr medium, *Optics Letters* **7**, 347-349 (1982).
72. P.W. Smith, A. Ashkin, and W.J. Tomlinson, Four-wave mixing in an artificial Kerr medium, *Optics Letters* **6**, 284-286 (1981).
73. P.W. Smith, *et al*., Studies of self-focusing bistable devices using liquid suspensions of dielectric particles, *Optics Letters* **9**, 131 – 133 (1984).
74. R. El-Ganainy, *et al*., Soliton dynamics and self-induced transparency in nonlinear nanosuspensions, *Optics Express* **15**, 10207-10218 (2007).
75. R. Gordon, J.T. Blakely and D. Sinton, Particle-optical self-trapping*, Physical Review A (Atomic, Molecular, and Optical Physics)* **75**, 055801-4 (2007).

76. P.J. Reece, E.M. Wright and K. Dholakia, Experimental observation of modulation instability and optical spatial soliton arrays in soft condensed matter, *Physical Review Letters* **98**, 203902 (2007).

77. M. Matuszewski, W. Krolikowski and Y.S. Kivshar, Soliton interactions and transformations in colloidal media, *Physical Review A (Atomic, Molecular, and Optical Physics)* **79**, 023814-6 (2009).

78. W.M. Lee, *et al.*, Nonlinear optical response of colloidal suspensions. *Optics Express* **17**, 10277-10289 (2009).

79. M.A. Go, P.N. Fung, H.A. Bachor, V.R. Daria, Optimal complex field holographic projection, *Optics Letters* **36**, 3073-3075 (2011).

80. J. Glückstad, Phase contrast image synthesis, *Opt. Commun.* **130**, 225-230 (1996)

81. J. Glückstad and P. Mogensen, Optimal phase contrast in common-path interferometry, *Applied Optics* **40**, 268-282 (2001).

82. V.R. Daria, R. Eriksen and J. Glückstad, Dynamic manipulation of aggregated structures using a spatial light modulator, *Journal of Modern Optics* **50**, 1601-1614, (2003)

83. J. Glückstad, D. Palima, P.J. Rodrigo, C.A. Alonzo, Laser projection using generalized phase contrast, *Optics Letters* **32**, 3281-83 (2007).

84. M.J. Romero and V.R. Daria, Modified filter design to optimize the synthetic reference wave in the generalized phase contrast method, *Optics Communications* **280**, 237-242 (2007).

85. D. Palima and V.R. Daria, Effect of spurious diffraction orders in arbitrary multi-foci patterns produced via phase-only holograms, *Applied Optics* **45**, 6689-6693 (2006).

86. P.J. Rodrigo, V.R. Daria, J. Glückstad, Four-dimensional optical manipulation of colloidal particles, *Applied Physics Letters* **86**, 074103 (2005).

87. M. Dienerowitz, M. Mazilu, P.J. Reece, T.F. Krauss and K. Dholakia, Optical vortex trap for resonant confinement of metal nanoparticles, *Optics Express* **16**, 4991–4999 (2008).

88. K. Sakai, K. Nomura, T. Yamamoto and K. Sasaki, Excitation of multiple plasmons by optical vortex beams, *Scientific Reports* **5**, 8431 (2015)

89. Z. Yan, *et al.*, Three-dimensional optical trapping and manipulation of single silver nanowires, *Nano Letters* **12**, 5155–5161 (2012).

90. S. Kawata and T. Sugiura, Movement of micrometer-sized particles in the evanescent field of a laser beam, *Optics Letters* **17**, 772–774 (1992).

91. C. Girard, A. Dereux and O.J.F. Martin, Theoretical analysis of light-inductive forces in scanning probe microscopy, *Physical Review B* **49**, 13872–13881 (1994).

92. A. Dereux, C. Girard, O.J.F. Martin and M. Devel, Optical binding in scanning probe microscopy, *Europhysics Letters* **26**, 37–42 (1994).

93. L. Novotny, R.X. Bian and X.S. Xie, Theory of nanometric optical tweezers, *Physical Review Letters* **79**, 645–648 (1997).

94. O.J.F. Martin and C. Girard, Controlling and tuning strong optical field gradients at a local probe microscope tip apex, *Applied Physics Letters* **70**, 705–707 (1997).

95. K. Okamoto and S. Kawata, Radiation force exerted on subwavelength particles near a nanoaperture, *Physical Review Letters* **83**, 4534–4537 (1999).

96. R. Quidant, D. Petrov and G. Badenes, Radiation forces on a Rayleigh dielectric sphere in a patterned optical near field, *Optics Letters* **30**, 1009–1011 (2005).

97. C. Pin, B. Cluzel, C. Renaut, E. Picard, D. Peyrade, E. Hadji and F. de Fornel, Optofluidic near-field optical microscopy: near-field mapping of a silicon nanocavity using trapped microbeads, *ACS Photonics* **2**, 1410-1415 (2015).

98. S. Kawata and T. Tani, Optically driven Mie particles in an evanescent field along a channelled waveguide, *Optics Letters* **21**, 1768–1770 (1996).

99. L.N. Ng, B.J. Luff, M.N. Zervas and J.S. Wilkinson, Propulsion of gold nanoparticles on optical waveguides, Optics Communications **208**, 117–124 (2002).

100. B.S. Ahluwalia, P. McCourt, T. Huser and O.G. Hellesø, Optical trapping and propulsion of red blood cells on waveguide surfaces, *Optics Express* **18**, 21053–21061 (2010).

101. B.S. Schmidt, A.H.J. Yang, D. Erickson and M. Lipson, Optofluidic trapping and transport on solid core waveguides within a microfluidic device, *Optics Express* **15**, 14322–14334 (2007).

102. A.H.J. Yang, S.D. Moore, B.S. Schmidt, M. Klug, M. Lipson, and D. Ericks on, Optical manipulation of nanoparticles and biomolecules in sub- wavelength slot waveguides, *Nature* **457**, 71–75 (2009).

103. V. Garcés-Chávez, K. Dholakia and G.C. Spalding, Extended-area optically induced organization of microparticles on a surface, *Applied Physics Letters* **86**, 031106 (2005).

104. M. Ploschner, T. Cizmar, M. Mazilu, A. Di Falco, K. Dholakia, Bidirectional optical sorting of gold nanoparticles, *Nano Letters* **12**, 1923–1927 (2012).

105. M. Juan, M. Righini, R. Quidant, Plasmon nano-optical tweezers, *Nature Photonics* **5**, 349-356 (2011).

106. J. Donner, G. Baffou, D. McCloskey and R. Quidant, Plasmon-assisted optofluidics, *ACS Nano* **5**, 5457-5462 (2011).
107. S. Barrow, X. Wei, J. Baldauf, A. Funston, P. Mulvaney, The surface plasmon modes of self-assembled gold nanocrystals, *Nature Communications* **3**, 1275 (2012).
108. G. Volpe, R. Quidant, G. Badenes and D. Petrov, Surface plasmon radiation forces. *Physical Review Letters* **96**, 238101 (2006).
109. G. Baffou and R. Quidant, Thermo-plasmonics: using metallic nanostructures as nano-sources of heat, *Laser Photonics Review* **7**, 171–187 (2013).
110. P.R. Huft, *et al*, Holographic Plasmonic Nanotweezers for Dynamic Trapping and Manipulation, *Nano Letters* **17**, 7920–7925 (2017).
111. W. Tsai, J.-S. Huang and C. Huang, Selective trapping or rotation of isotropic dielectric microparticles by optical near field in a plasmonic Archimedes spiral, *Nano Letters* **14**, 547–552 (2014).
112. L. Shao, Z.-J. Yang, D. Andrén, P. Johansson and M. Käll, Gold nanorod rotary motors driven by resonant light scattering, *ACS Nano* **9**, 12542-12551 (2015).
113. K. Wang, E. Schonbrun, P. Steinvurzel and K.B. Crozier, Trapping and rotating nanoparticles using a plasmonic nano-tweezer with an integrated heat sink, *Nature Communications* **2**, 469 (2011).
114. G.H. Yuan, Q. Wang, P.S. Tan and X.-C. Yuan, A dynamic plasmonic technique assisted by phase modulation of an incident optical vortex beam, Nanotechnology 23, 385204 (2012).
115. C. Min, *et al*., Focused plasmonic trapping of metallic particles, *Nature Communications* **4**, 7 (2013)
116. K. Wang, E. Schonbrun and K.B. Crozier, Propulsion of gold nanoparticles with surface plasmon polaritons: evidence of enhanced optical force from near-field coupling between gold particle and gold Film, *Nano Lett*ers **9**, 2623–2629 (2009).
117. A. Cuche, O. Mahboub, E. Devaux, C. Genet, T.W. Ebbesen, Plasmonic coherent drive of an optical trap, *Physical Review Letters* **108**, 26801 (2012).
118. A. Cuche, B. Stein, A. Canguier-Durand, E. Devaux, C. Genet, T.W. Ebbesen, Brownian motion in a designer force field: Dynamical effects of negative refraction on nanoparticles, *Nano Letters* **12**, 4329−4332 (2012).
119. K.Y. Chen, A.T. Lee, C.C. Hung, J.S. Huang, Y.T. Yang, Transport and trapping in two-dimensional nanoscale plasmonic optical lattice, *Nano Letters* **13**, 4118–4122 (2013).
120. M.A. Go and V.R. Daria, Light-Neuron interactions: key to understanding the brain, *Journal of Optics* **19**, 23002 (2017).
121. M.A. Go, J.M.C. Choy, A. Colibaba, S. Redman, H.A. Bachor, C. Stricker and V.R. Daria, Targeted pruning of a neuron's dendritic tree via femtosecond laser dendrotomy, *Scientific Reports* **6**, 19078 (2016).
122. J. Ando, G. Bautista, N. Smith, K. Fujita and V.R. Daria, Optical trapping and surgery of living yeast cells using a single laser, *Review of Scientific Instruments* **79**, 103705 (2008).
123. MA Taylor, J Janousek, VR Daria, J. Knittel, B. Hage, HA Bachor, WP Bowen, Subdiffraction-limited Quantum Imaging within a living cell, *Physical Review X* **4**, 011017 (2014).
124. MA Taylor, J Janousek, VR Daria, J. Knittel, B. Hage, HA Bachor, WP Bowen, Biological measurement beyond the quantum limit, *Nature Photonics* **7**, p229 (2013).
125. M. Iwaki, A.H. Iwane, K. Ikezaki and T. Yanagida, Local heat activation of single myosins based on optical trapping of gold nanoparticles, *Nano Letters* **15**, 2456–2461 (2015).
126. A.S. Urban, *et al*., Controlled nanometric phase transitions of phospholipid membranes by plasmonic heating of single gold nanoparticles, *Nano Letters* **9**, 2903-2908 (2009).
127. M.G. Shapiro, *et al*., Infrared light excites cells by changing their electrical capacitance, *Nature Communications* **3**, 736 (2012).
128. H. Nakatsuji, *et al*., Thermosensitive ion channel activation in single neuronal cells by using surface-engineered plasmonic nanoparticles, *Angewandte Chemie International Edition* **54**, 11725-11729 (2015).
129. J. Yong, *et al*., Gold-nanorod-assisted near-infrared stimulation of primary auditory neurons, *Advanced Healthcare Materials* **3**, 1862-1868 (2014).
130. K. Eom, *et al*., Enhanced infrared neural stimulation using localized surface plasmon resonance of gold nanorods, *Small* **10**, 3853-3857 (2014).
131. J.L. Carvalho-de-Souza, *et al*., Photosensitivity of neurons enabled by cell-targeted gold nanoparticles, *Neuron* **86**, 207-217 (2015).
132. N. Farah, *et al*., Holographically patterned activation using photo-absorber induced neural-thermal stimulation, *Journal of Neural Engineering* **10**, 56004 (2013).
133. C. Paviolo, *et al*., Laser exposure of gold nanorods can induce intracellular calcium transients, *Journal of Biophotonics* **7**, 761-765 (2014).

134. A. Ehrlicher, *et al*., Guiding neuronal growth with light, *Proceedings of the National Academy of Science USA* **99**, 16024-16028 (2002).
135. C. Hosokawa, S.N. Kudoh, A. Kiyohara and T. Taguchi, Optical trapping of synaptic vesicles in neurons, *Applied Physics Letters* **98**, 163705 (2011).
136. P.D. Chowdary, *et al*., Nanoparticle-assisted optical tethering of endosomes reveals the cooperative function of dyneins in retrograde axonal transport, *Scientific Reports* **5**, 18059 (2015).
137. I.A. Favre-Bulle, A.B. Stilgoe, H. Rubinsztein-Dunlop and E.K. Scott, Optical trapping of otoliths drives vestibular behaviours in larval zebrafish, *Nature Communications* **8**, 630 (2017).
138. M.-C. Zhong, X.-B. Wei, J.-H. Zhou, Z.-Q. Wang & Y.-M. Li, Trapping red blood cells in living animals using optical tweezers, Nature Communications 4, 1768 (2013).
139. L.M. Browning, T. Huang, and X.-H. Nancy Xu, Real-time *in vivo* imaging of size-dependent transport and toxicity of gold nanoparticles in zebrafish embryos using single nanoparticle plasmonic spectroscopy, *Interface Focus* **3**, 20120098 (2013).
140. K.J. Lee, P.D. Nallathamby, L.M. Browning, C.J. Osgood and X.-H.N. Xu, *In Vivo* imaging of transport and biocompatibility of single silver nanoparticles in early development of zebrafish embryos, *ACS Nano* **1**, 133–143 (2007).
141. S. Böhme, M. Baccaro, M. Schmidt, A. Potthoff, H.-J. Stärk, T. Reemtsma and D. Kühnel, Metal uptake and distribution in the zebrafish (Danio rerio) embryo: differences between nanoparticles and metal ions, *Environmental Science: Nano* **4**, 1005-1015 (2017).